ATMOSPHERIC AND OCEANIC SCIENCE LETTERS, 2010, VOL. 3, NO. 1, 25–30

The Formation of Precipitation Anomaly Patterns during the Developing and Decaying Phases of ENSO

HU Kai-Ming and HUANG Gang

State Key Laboratory of Numerical Modeling for Atmospheric Sciences and Geophysical Fluid Dynamics, Institute of Atmospheric Physics, Chinese Academy of Sciences, Beijing 100029, China

Received 20 September 2009; revised 17 December 2009; accepted 22 December 2009; published 16 January 2010

Abstract This study proposes a new explanation for the formation of precipitation anomaly patterns in the boreal summer during the El Niño-Southern Oscillation (ENSO) developing and decaying phases. During the boreal summer June-July-August (JJA) (0) of the El Niño (La Niña) developing phase, the upper level (300–100 hPa) positive potential temperature anomalies resemble a Matsuno-Gill-type response to central Pacific heating (cooling), and the lower level (1000–850 hPa) potential temperature anomalies are consistent with local SST anomalies. During the boreal summer JJA(1) of the El Niño (La Niña) decaying phase, the upper level potential temperature warms over the entire tropical zone and resembles a Matsuno-Gill-type response to Indian Ocean heating (cooling), and the lower level potential temperature anomalies follow local SST anomalies. The vertical heterogeneity of potential temperature anomalies influences the atmospheric stability, which in turn influences the precipitation anomaly pattern. The results of numerical experiments confirm our observations.

Keywords: precipitation pattern, ENSO, AGCM

Citation: Hu, K.-M., and G. Huang, 2010: The formation of precipitation anomaly patterns during the developing and decaying phases of ENSO, *Atmos. Oceanic Sci. Lett.*, **3**, 25–30.

1 Introduction

It is now well recognized that the El Niño-Southern Oscillation (ENSO) phenomenon is a dominant mode of tropical climate variability (e.g., Bjerknes, 1969). The boreal summer rainfall anomalies associated with ENSO are of great socio-economic importance; for example, they can influence the Indian summer monsoon (e.g., Kumar et al., 1999), the Australia summer monsoon (e.g., Wu and Kirtman, 2007), the East Asia summer monsoon (e.g., Huang and Wu, 1989; Wu et al., 2003), and the western North Pacific summer monsoon (e.g., Li et al., 2008; Wang et al., 2001; Wu and Wang, 2000; Xie et al., 2009; Yang et al., 2007).

Previous studies show that the anomalous precipitation pattern not only depends on sea surface temperature (SST), but it is also influenced by large-scale atmospheric circulation (e.g., Lau et al., 1997). On the other hand, the tropical convection anomaly can also influence atmospheric circulation (e.g., Gill, 1980; Matsuno, 1966; Xie et al., 2009). Thus, SST, precipitation, and atmospheric circulation have all been shown to interact with each other. In this paper, we propose a new idea to describe the formation of the anomalous precipitation pattern in the boreal summer during the El Niño (La Niña) developing and decaying phases.

While El Niño (La Niña) is developing, the central and eastern tropical Pacific SST becomes warmer (cooler) during the boreal summer. While El Niño (La Niña) is decaying, the central and eastern tropical Pacific SST returns to normal, but the Indian Ocean and Atlantic SST become warmer (cooler) because of the atmospheric bridge (e.g., Klein et al., 1999; Lau and Nath, 2003) and ocean Rossby wave (e.g., Du et al., 2009; Huang and Kinter, 2002; Xie et al., 2002). The present study illustrates that there is a Matsuno-Gill-type response (e.g., Gill, 1980; Matsuno, 1966; Su and Neelin, 2003) to the central and eastern tropical SST warming (cooling) during the June-July-August (JJA) (0) period and to the tropical Indian Ocean warming (cooling) during the JJA(1) period (e.g., Li et al., 2008; Wu et al., 2009; Xie et al., 2009; Yang et al., 2007). Upper level temperature anomalies can propagate to remote regions through atmospheric waves. The lower level atmospheric temperature anomalies are more constrained by local SST anomalies, which may result from the direct heat exchange between the ocean and atmosphere. Therefore, the atmospheric warming (cooling) is not homogeneous from the lower level to upper level. Moreover, the vertical heterogeneity of temperature anomalies may influence the atmospheric stability and in turn rainfall during JJA(0) and JJA(1).

The goal of this paper is to study the formation of the precipitation anomaly pattern during the developing phase and decaying phases of ENSO. The remainder of the paper is organized into sections: the second section describes the data and methods used; the third section presents our analysis of the observations and model simulations; and the last section provides a summary and the discussion.

2 Data and experiment

2.1 Data

We used the Hadley center SST (HadSST) dataset (e.g., Rayner et al., 2003) and the National Centers for Environmental Prediction (NCEP) atmospheric reanalysis (e.g.,

Corresponding author: HUANG Gang, hg@mail.iap.ac.cn

Kalnay et al., 1996), which were originally on 1° and 2.5° grids, respectively. The CPC (Climate Prediction Center) Merged Analysis of Precipitation (CMAP) precipitation data (e.g., Xie and Arkin, 1997) were used as a proxy for observations. For consistency with the precipitation data, all observation analyses and model data were based on the 1979–2000 period. Over the 22-year time series, a correlation coefficient of 0.44 reached the 95% significance level based on the Student *t*-test.

The atmospheric stability (AS) was calculated as the upper level (300–100 hPa) potential temperature minus the lower level (1000–850 hPa) potential temperature. We used the SST averaged over the eastern equatorial Pacific (Niño3.4: 5°S–5°N, 120–170°W) as the ENSO index.

2.2 Model

The Community Atmosphere Model Version3 (CAM3) at T42 resolution (about 2.8° latitude × 2.8° longitude) in the horizontal and 23 sigma levels in the vertical was used in this study. Details of the physical and numerical methods used in CAM3 are provided in Collins et al. (2006). We performed a 21-member ensemble of the CAM3 model integration forced by the observed monthly mean SSTs from the Hadley Center dataset during the 1950–2000 period, which we designate CAM3_EM. The members of the ensemble for CAM3_REAL differ only in their initial conditions. Results of model simulations are based on the 21-member ensemble mean.

3 Results

The JJA(0) (JJA(1)) correlation distribution of both precipitation and atmospheric stability with the December-January-February (DJF) (0) Niño3.4 index is shown in Fig. 1a (Fig. 1c). The results apply to both El Niño and La Niña; however, the rest of this paper only describes the anomalies corresponding to the El Niño cases because the La Niña cases are the same as for El Niño, except the sign is reversed. During JJA(0), more rainfall is seen in the positive AS-Niño3.4 (atmospheric stability with Niño3.4 index) correlation region, which is mainly located in the central-eastern tropical Pacific and South Atlantic; less rainfall is seen in the negative AS-Niño3.4 correlation region, which is mainly over the east of Australia, southwestern Pacific, and tropical Atlantic (Fig. 1a). During JJA(1), the tropical atmospheric stability increases over almost the entire tropical zone, except over the western Indian Ocean and the eastern Pacific. Rainfall decreases in regions where higher positive AS-Niño3.4 correlations are seen, such as in the subtropical North Pacific, tropical South Atlantic, and a belt from eastern Australia to southern South America; rainfall increases in regions of negative or low positive AS-Niño3.4 correlations, which for example occurs in the western Indian Ocean and in the central and eastern Pacific (Fig. 1c). The model results are consistent with the observations (Figs. 1b and 1d). There are some regions where the rainfall increase (decrease) does not coincide with an atmospheric stability decrease (increase), such as in the North Pacific where there is more rainfall during JJA(0) but atmospheric stability increases. Figure 1 demonstrates that atmospheric stability can impact rainfall anomalies, however, this question remains: how does the atmospheric stability anomaly pattern forms in the boreal summer during the El Niño developing and decaying phases?

Previous studies show that the local SST can impact remote regions through atmosphere waves, which can in turn impact the upper-level atmospheric temperature (e.g., Su and Neelin, 2003; Xie et al., 2009). We calculated the correlation of the upper level (300–100 hPa) potential temperature anomaly with the DJF Niño3.4 index, which is shown in Fig. 2. The distribution of the upper level po-

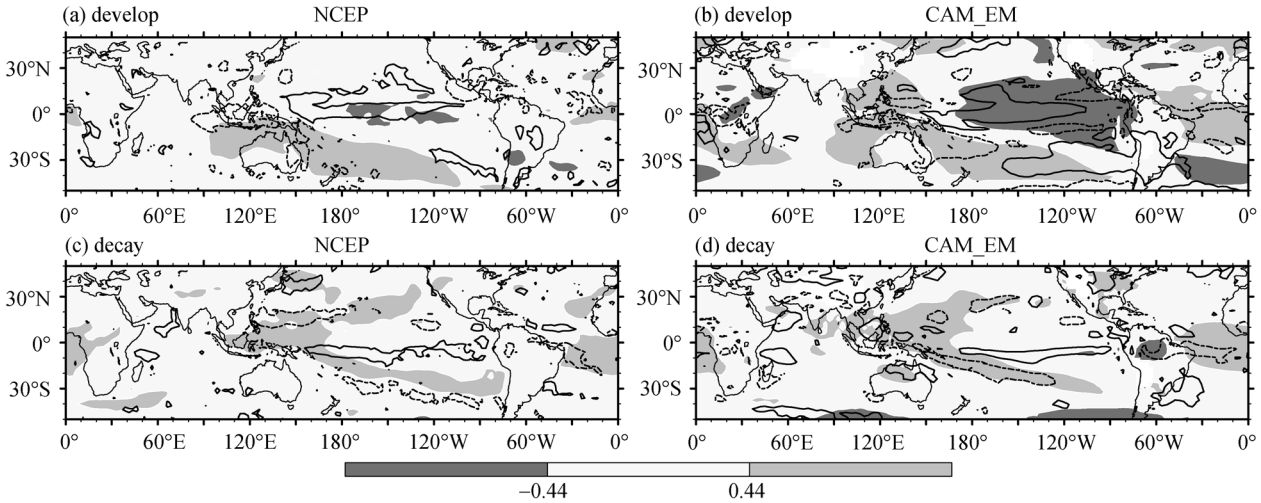

Figure 1 Correlations of DJF mean Niño3.4 index with precipitation (lines) (the dashed line denotes a correlation coefficient below –0.44, and the solid line denotes a correlation coefficient above 0.44) and with atmospheric stability (shading) during (a) the preceding JJA(0) and (c) the following JJA(1). Plots (b) and (d) are the same as (a) and (c) but use ensemble means from the CAM3 experiment. Both the computation of observed correlations and the simulation analysis of the 21-member ensemble mean were based on the same 22 years of data (1979–2000).

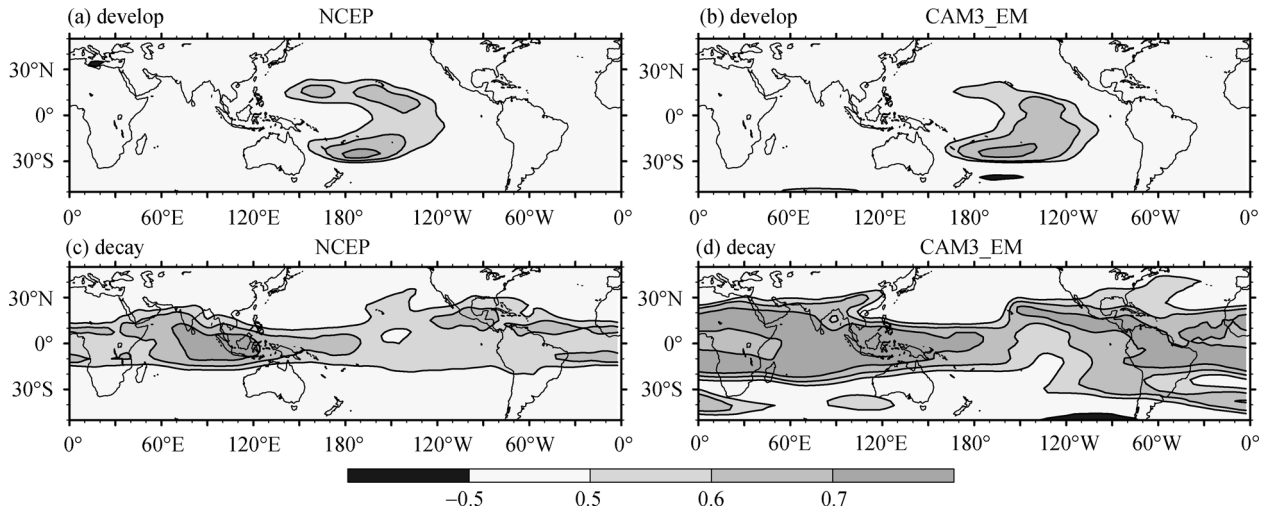

Figure 2 Correlation coefficients between the DJF mean Niño3.4 index and the upper level (300–100 hPa) vertically averaged potential temperature during (a) the preceding JJA(0) and (c) the following JJA(1). Plots (b) and (d) are the same as Figs. 1a and 1c, but use ensemble means from the CAM3 experiment. Both the computation of observed correlations and the simulation analysis of the 21-member ensemble mean were based on the same 22 years of data (1979–2000).

tential temperature-Niño3.4 correlation displays a Gill-type response to the central Pacific atmospheric heating, and the anomalies are mainly concentrated on the Pacific during JJA(0). During JJA(1), the potential temperature increases along the entire tropical zone and features a Matsuno-Gill-type response to SST warming in the Indian Ocean, which is consistent with previous studies. The model results are the similar as the observations. It is unclear why the upper level potential temperature-Niño3.4 correlation is mainly confined to the Pacific during JJA(0) but covers the entire tropical zone during JJA(1). This may be because of the difference in the SST anomalies between JJA(0) and JJA(1). As Fig. 3 shows, positive SST anomalies are mainly concentrated in the tropical Pacific during JJA(0), but they are found in the entire tropical ocean during JJA(1).

The distribution of lower level potential temperature anomalies is the same as that of local SST anomalies during both JJA(0) and JJA(1) (Figs. 4a and 4c). There are positive anomalies over the central-eastern Pacific and

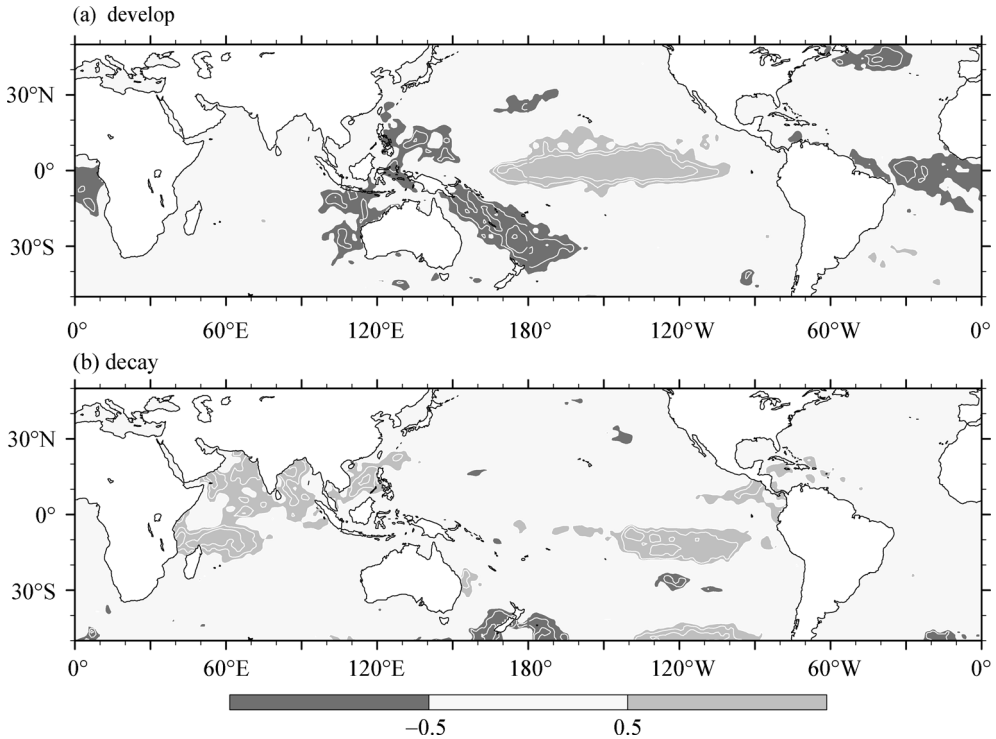

Figure 3 Correlation coefficient between the DJF mean Niño3.4 index and sea surface temperature (white contours at intervals of 0.1; dark shade<–0.5; light>0.5) during (a) JJA(0) and (b) JJA(1) from 1979 to 2000.

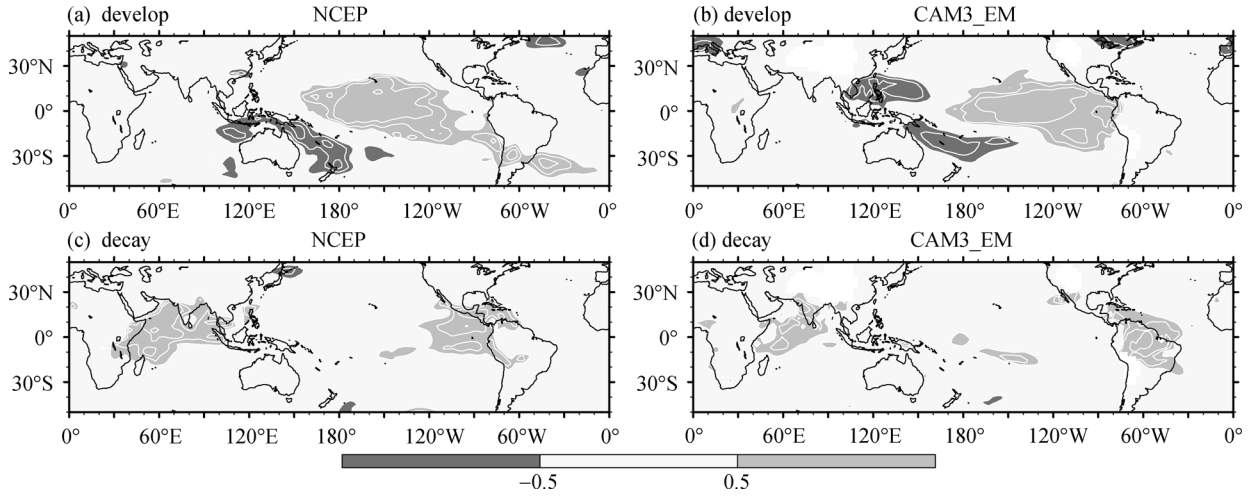

Figure 4 Correlation coefficient between the DJF mean Niño3.4 index and the lower level (1000–850 hPa) vertically averaged potential temperature (white contours at intervals of 0.1; dark shade<–0.5; light>0.5) during (a) the preceding JJA(0) and (c) the following JJA(1). Plots (b) and (d) are the same as Figs. 1a and 1c, but use ensemble means from the CAM3 experiment. Both the computation of observed correlations and the simulation analysis of the 21-member ensemble mean were based on the same 22 years of data (1979–2000).

negative anomalies over the western Pacific during JJA(0); positive anomalies are found over the Indian Ocean, central Pacific, and equatorial America during JJA(1). The model results, as shown in Figs. 4b and 4d, are consistent with the observations. The similar distribution of lower level potential temperature anomalies and SST anomalies may result from the direct air-sea heat exchange.

The results show that lower level potential temperature anomalies are constrained most strongly by the local SST, whereas the upper level potential temperature anomalies are influenced by atmospheric waves. Thus, potential temperature anomalies are vertically heterogeneous, which can influence the atmospheric stability and in turn influence the precipitation anomalies in the boreal summer during the El Niño developing and decaying phases.

4 Summary and discussion

In the boreal summer, during the developing phase of El Niño (La Niña), the SST anomalies occur mainly in the tropical Pacific. The upper level temperature anomaly pattern resembles a Gill-type response to the central Pacific warming (cooling); the lower level temperature anomaly pattern is consistent with the SST anomaly distribution. The heterogeneous vertical distributions of potential temperature change the atmospheric stability, which can influence the tropical rainfall in JJA(0). In the boreal summer, during the El Niño (La Niña) decaying phase, the upper-level temperature anomalies resemble a Matsuno-Gill-type response to the Indian Ocean heating (cooling); the lower level potential anomalies are mainly constrained by local SST anomalies. Numerical experiment results confirm these observations. The heterogeneous potential temperature distributions lead to a change in atmospheric stability, which can influence the tropical rainfall.

Although the distribution of the precipitation-Niño3.4 correlation and atmospheric stability-Niño3.4 correlation coincide with each other in most regions, there are also some regions where they do not. This disagreement may be caused by other processes that lead to precipitation anomalies, such as low-level atmospheric circulation, moisture flux, etc. As in Fig. 1, we calculated the JJA(0) (JJA(1)) correlation coefficient of both precipitation and the 10-m-layer convergence with the DJF(0) Niño3.4 index for Fig. 5a (Fig. 5b), which shows that although the correlation distribution between the 10-m-layer convergence and the Niño3.4 index is scattered, we do find more (less) rainfall over the positive (negative) correlation regions. It is interesting that the JJA(1) rainfall anomalies over the western North Pacific correspond to low-layer convergence but are not consistent with atmospheric instability.

Previous studies have shown that ENSO decayed quickly in the boreal spring before the late 1970s but has decayed slowly after the late 1970s (e.g., Wang et al., 2008). In addition, the pattern of SST anomalies in the summer during ENSO decaying periods has experienced a decadal change since the late 1970s (e.g., Xie et al., 2010[1]). Whether the precipitation anomaly pattern in the boreal summer during the ENSO developing and decaying phases has changed is an interesting question that needs further study.

[1] Xie, S. P., Y. Du, G. Huang, et al., 2010: Interdecadal change of the 1970s in El Niño influences interdecadal change of the 1970s in El Niño influences, submitted to *J. Climate*.

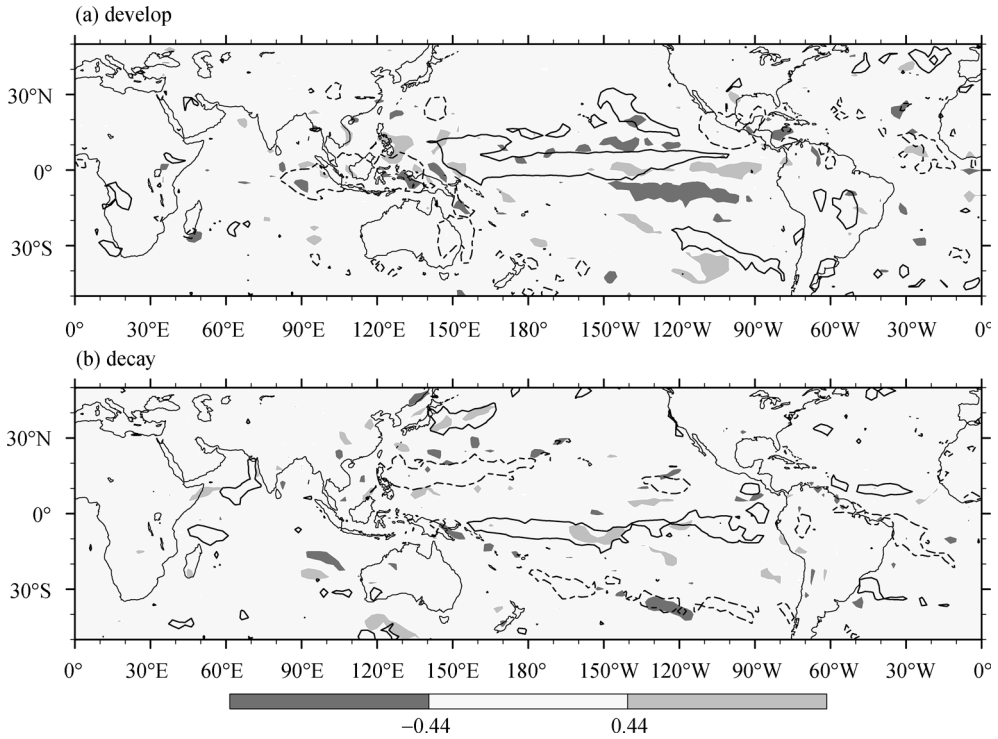

Figure 5 Correlation of (DJF) mean Niño3.4 index with precipitation (lines) (dashed line denotes a correlation coefficient below −0.44, and solid line denotes a correlation coefficient above 0.44) and with the 10-m-layer wind convergence (shading) during (a) the preceding JJA(0) and (b) the following JJA(1).

Acknowledgements. The authors thank two anonymous reviewers for their constructive comments that helped improve this manuscript. This work is supported by the National Basic Research Program of China (2006CB400503), the National Natural Science Foundation of China (40890155, 40775051, and U0733002), and Project KZCX2-YW-220 of the Chinese Academy of Sciences.

References

Bjerknes, J., 1969: Atmospheric teleconnections from the equatorial Pacific, *Mon. Wea. Rev.*, **97**, 163−172.

Collins, W. D., C. M. Bitz, M. L. Blackmon, et al., 2006: The Community Climate System Model version 3 (CCSM3), *J. Climate*, **19**, 2122−2143.

Du, Y., S.-P. Xie, G. Huang, et al., 2009: Role of air-sea interaction in the long persistence of El Niño-induced North Indian Ocean warming, *J. Climate*, **22**, 2023−2038.

Gill, A. E., 1980: Some simple solutions for heat-induced tropical circulation, *Quart. J. Roy. Meteor. Soc.*, **106**, 447−462.

Huang, B. H., and J. L. Kinter, 2002: Interannual variability in the tropical Indian Ocean, *J. Geophys. Res.*, **107**, 3199, doi:10.1029/2001JC001278.

Huang, R., and Y. Wu, 1989: The influence of ENSO on the summer climate change in China and its mechanism, *Adv. Atmos. Sci.*, **6**, 21−32.

Kalnay, E., M. Kanamitsu, R. Kistler, et al., 1996: The NCEP/NCAR 40-year reanalysis project, *Bull. Amer. Meteor. Soc.*, **77**, 437−471.

Klein, S. A., B. J. Soden, and N. C. Lau, 1999: Remote sea surface temperature variations during ENSO: Evidence for a tropical atmospheric bridge, *J. Climate*, **12**, 917−932.

Kumar, K. K., B. Rajagopalan, and M. A. Cane, 1999: On the weakening relationship between the Indian Monsoon and ENSO, *Science*, **284**, 2156−2159.

Lau, K. M., H. T. Wu, and S. Bony, 1997: The role of large-scale atmospheric circulation in the relationship between tropical convection and sea surface temperature, *J. Climate*, **10**, 381−392.

Lau, N. C., and M. J. Nath, 2003: Atmosphere-ocean variations in the Indo-Pacific sector during ENSO episodes, *J. Climate*, **16**, 3−20.

Li, S., J. Lu, G. Huang, et al., 2008: Tropical Indian Ocean basin warming and East Asian summer monsoon: A multiple AGCM study, *J. Climate*, **21**, 6080−6088.

Matsuno, T., 1966: Quasi-geostrophic motions in the equatorial area, *J. Meteor. Soc. Japan*, **44**, 25−43.

Rayner, N. A., D. E. Parker, E. B. Horton, et al., 2003: Global analyses of sea surface temperature, sea ice, and night marine air temperature since the late nineteenth century, *J. Geophys. Res.*, **108**, 4407, doi:10.1029/2002JD002670.

Su, H., and J. D. Neelin, 2003: The scatter in tropical average precipitation anomalies. *J. Climate*, **16**, 3966−3977.

Wang, B., R. G. Wu, and K. M. Lau, 2001: Interannual variability of the Asian summer monsoon: Contrasts between the Indian and the western North Pacific-east Asian monsoons, *J. Climate*, **14**, 4073−4090.

Wang, B., J. Yang, and T. J. Zhou, 2008: Interdecadal changes in the major modes of Asian-Australian monsoon variability: Strengthening relationship with ENSO since the late 1970s, *J. Climate*, **21**, 1771−1789.

Wu, B., T. J. Zhou, and T. Li, 2009: Seasonally evolving dominant interannual variability modes of East Asian climate, *J. Climate*, **22**, 2992−3005.

Wu, R., and B. P. Kirtman, 2007: Roles of the Indian Ocean in the Australian summer monsoon-ENSO relationship, *J. Climate*, **20**, 4768−4788.

Wu, R., and B. Wang, 2000: Interannual variability of summer monsoon onset over the western North Pacific and the underlying processes, *J. Climate*, **13**, 2483−2501.

Wu, R. G., Z. Z. Hu, and B. P. Kirtman, 2003: Evolution of ENSO-related rainfall anomalies in East Asia, *J. Climate*, **16**, 3742−3758.

Xie, P., and P. A. Arkin, 1997: Global Precipitation: A 17-year

monthly analysis based on gauge observations, satellite estimates, and numerical model outputs, *Bull. Amer. Meteor. Soc.*, **78**, 2539–2558.

Xie, S. P., H. Annamalai, F. A. Schott, et al., 2002: Structure and mechanisms of South Indian Ocean climate variability, *J. Climate*, **15**, 864–878.

Xie, S. P., K. M. Hu, J. Hafner, et al., 2009: Indian Ocean Capacitor Effect on Indo-western Pacific climate during the summer following El Niño, *J. Climate*, **22**, 730–747.

Yang, J. L., Q. Y. Liu, S. P. Xie, et al., 2007: Impact of the Indian Ocean SST basin mode on the Asian summer monsoon, *Geophys. Res. Lett.*, **34**, L02708, doi:10.1029/2006GL028571.